Research Article

Journal of CHEMOMETRICS

Received: 28 September 2007, Accepted: 3 October 2007, Published online in Wiley InterScience: 2008

(www.interscience.wiley.com) DOI: 10.1002/cem.1099

Use of local rank-based spatial information for resolution of spectroscopic images

Anna de Juan[a]*, Marcel Maeder[b], Thomas Hancewicz[c] and Romà Tauler[d]

Spectroscopic images are singular chemical measurements that enclose chemical and spatial information about samples. Resolution of spectroscopic images is focused on the recovery of the pure spectra and distribution maps of the image constituents from the sole raw spectroscopic measurement. In image resolution, constraints are generally limited to non-negativity and the spatial information is generally not used. Local rank analysis methods have been adapted to describe the local spatial complexity of an image, providing specific pixel information. This local rank information combined with reference spectral information allows the identification of absent compounds in pixels with low compound overlap. The introduction of this information in the resolution process under the form of constraints helps to increase the performance of the resolution method and to decrease the ambiguity linked to the final solutions. Copyright © 2008 John Wiley & Sons, Ltd.

Manuscript in memoriam of Professor D.L. Massart

Keywords: image analysis; curve resolution; MCR; local rank; constraints

1. INTRODUCTION

Spectroscopic images are defined by three informative directions: the spectral direction and two spatial directions, related to the *x*- and *y*-coordinates of each pixel. Thus, the spectra collected in each pixel characterize chemically the constituents of the image and this information and the pixel position in the sample provide a spatial-related compositional description of the sample [1,2]. Images are often displayed as cubes ($x \times y \times \lambda$), but their mathematical description does not require a three-dimensional model. Indeed, as any other spectroscopic measurement, all the pixels in an image obey the Beer–Lambert law, which translates into a bilinear model [3,4]. To visualize and compute this model, the original image cube should be unfolded into a data matrix (see Figure 1a). As a consequence, the concept of pixel neighborhood is partially lost because the transformation of the *x*- and *y*-coordinates of a pixel into a single dimension in the data matrix does not allow a pixel to be surrounded by all its neighbors in the original image. The bilinear model is easily understood once the image is unfolded. Thus, the original mixed measurement is described as the sum of the signal contribution of the different components ($\mathbf{D_A}$ and $\mathbf{D_B}$ for a two-component image in Figure 1a). Each one of these pure signal contributions can be expressed by a dyad of profiles: $\mathbf{s}_i$, the pure unit spectrum of the *i*th constituent, and $\mathbf{c}_i$, which weights the contribution of this particular component along the pixel direction (see Figure 1b). To recover the distribution map of a particular component, the stretched concentration profile, $\mathbf{c}_i$, should be refolded recovering the 2D structure of the original image. Figure 1c shows the typical matrix form of a bilinear model, $\mathbf{D} = \mathbf{CS}^T$, where the columns in matrix $\mathbf{C}$ contain the stretched concentration profiles of the pure components of an image and the rows of $\mathbf{S}^T$, their related pure spectra.

The goal resolution methods in image analysis is of recovering the pure spectra and distribution maps of the constituents of an image from the sole spectroscopic measurement, that is, recovering the pure profiles in the underlying bilinear model. Several methodologies can be found for this purpose. Some of them perform a selection of the purest pixels in the image [5–8], assign them to be the matrix $\mathbf{S}^T$ and derive the distribution maps, $\mathbf{C}$, in a single least squares step. Several iterative resolution methods [9–11] take this prior selection as an initial estimate of $\mathbf{S}^T$ to be refined through an iterative alternating least squares process under the action of constraints. This second option is much more powerful when there is no guarantee that we can find selective pixels for each particular constituent in the image. Constraints are essential to drive the iterative resolution process to chemically meaningful solutions and to decrease the rotational ambiguity inherent to the resolution results. However, this field has not been much explored in image analysis and non-negativity in the concentration and, when possible, in the spectral direction, is practically the only constraint generally applied [7,9–14]. A possible explanation of the scarce application of constraints in image analysis is the fact that most of the available constraints are designed for process analysis, where

* *Chemometrics Group, Department of Analytical Chemistry, Diagonal 647, 08028 Barcelona, Spain.*
E-mail: anna.dejuan@ub.edu

a *A. de Juan*
Chemometrics Group, Department of Analytical Chemistry, Diagonal 647, 08028 Barcelona, Spain

b *M. Maeder*
Department of Chemistry, The University of Newcastle, Callaghan, NSW 2308, Australia

c *T. Hancewicz*
Unilever Research & Development, Trumbull, 40 Merritt Blvd, Trumbull, CT 06611, USA

d *R. Tauler*
Department of Environmental Chemistry, Institute of Chemistry and Environmental Research, CSIC, Jordi Girona 18, 08034 Barcelona, Spain

This article was due to appear in the Massart Special Issue **21***(7–9).*

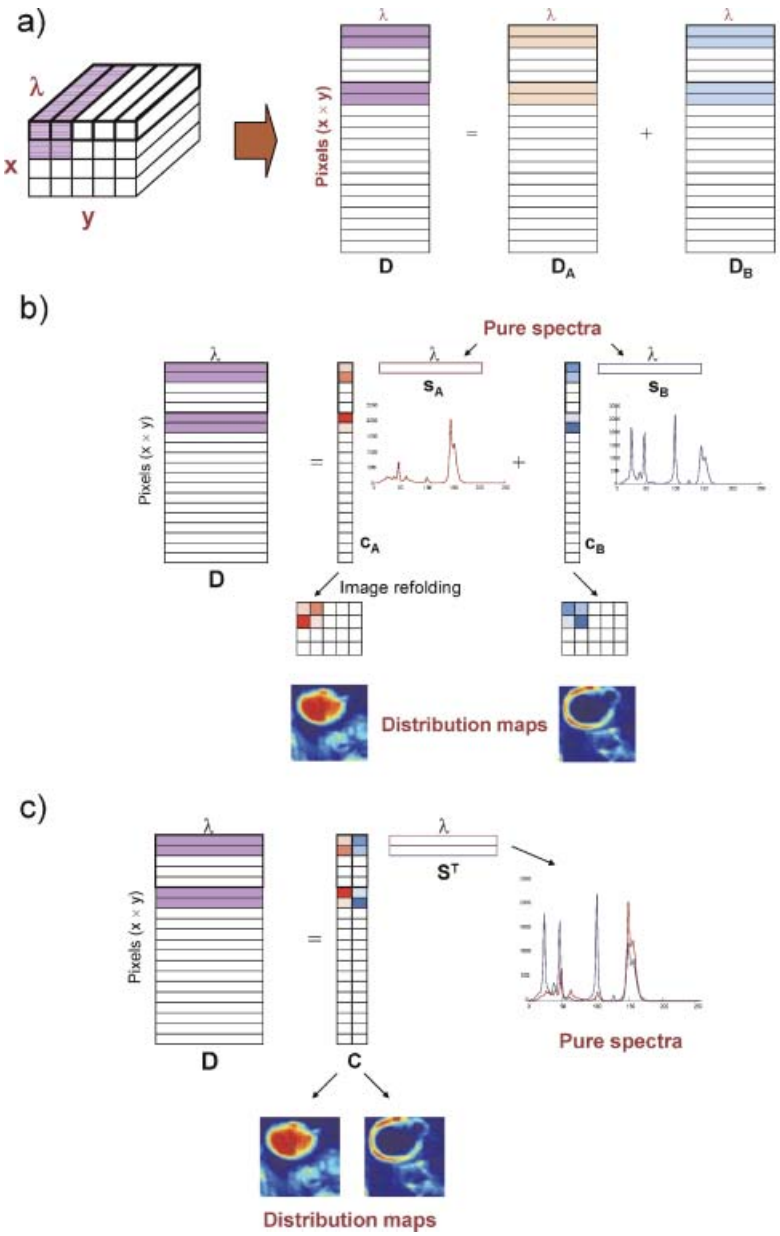

Figure 1. Image bilinear model. (a) Unfolding of cube image and decomposition in sum of pure component signal contributions. (b) Decomposition in sum of dyads of concentration profiles (stretched distribution maps) and pure spectra. (c) Bilinear image model in matrix form. This figure is available in color online at www.interscience.wiley.com/journal/cem

profiles tend to show a continuous smooth evolution, very different from the unpatterned stretched concentration profiles in an image. This lack of pattern stems from the natural heterogeneity of the image and from the fact that the original 2D pattern, if existing, is destroyed when the unfolding step is carried out.

At this point, we should think of adapting or designing new constraints that can take advantage of the image structure. If general constraints that describe the global shape of a concentration profile cannot be easily found, we may envision the use of information that affects pixels individually or local pixel areas. Very few attempts have been done in this direction. Taking into account the local compositional correlation between a pixel and its 2D neighbors for a particular constituent, a local smoothness constraint has been proposed [15]. Concerning the incorporation of pixel-specific knowledge, we can only mention a constraint related to set the identity of the components that should be found in a pixel from the prior application of a pixel classification method on the image to be resolved [16].

This work proposes for the first time the introduction of selectivity and local rank constraints in the resolution of spectroscopic images, that is, the use of the information related to the absence of certain components in particular pixels. Actually, selectivity and local rank constraints are among the most powerful to decrease the rotational ambiguity in resolution results [3,4,17,18]. These constraints have been applied since long in sequential processes because the output of local rank analyses allows for a straightforward identification of the missing components in the different local rank windows. In spectroscopic images, the unpatterned distribution of components prevents

the straight correspondence between local rank information and compound identity. This missing connection will be established through the combined use of Fixed Size Image Window-Evolving Factor Analysis (FSIW-EFA), a local rank analysis method specifically designed for spectroscopic image analysis [19], with some reference spectral information. The knowledge obtained on the number and identity of the absent components in particular pixels will be later coded under the form of local rank constraints. The methodology used to set this kind of constraint and the benefits from its application to obtain best-defined images and less ambiguous profiles will be shown in a real example of an emulsion image.

2. DATA SET

The image studied comes from an oil-in-water emulsion sample analyzed using a modified Raman imaging spectrometer from Instruments SA Explorer 1, which enables optical microscopy in all common contrast modes (using a simple CCD video camera and frame grabber). Details of the experimental setup are described elsewhere [19]. The data were collected using 633 nm excitation. Raman intensities were registered in the Raman shift range between 950–1800 cm^{-1}. The surface emulsion sample is formed by 60×60 pixels at 1 μm step size. Each of the 3600 spectra were composed of 253 points making the entire data set 910 800 data points [20,21].

The composition of the surface image has been described in previous works [20,21] and it is formed by a background phase and distinct drops of the oily phase. Four spectral components are present in these images. Two represent pure chemical components while the remaining two represent multicomponent phases that behave as a single component and are characteristic of these types of emulsion systems.

3. METHODOLOGY AND RESULTS

This section is devoted to show the protocol followed in the resolution of spectroscopic images when local rank constraints are introduced. There are two separate steps: the first one, oriented to gather the necessary local rank and reference spectral information and the second one, where this information is coded in the form of constraint and resolution is carried out. Since the working procedure of the chemometric methods and the interpretation of results is explained taking as example the real emulsion image, we have preferred to keep a unified section to avoid the unnecessary repetitions that would appear if Methods and Results were described separately. All the methods of this section have been implemented by the authors in a set of MATLAB routines, which are available on request.

3.1. Image local rank information

In order to set selectivity or local rank constraints in the resolution of an image, the necessary pixel-to-pixel local rank information will be obtained by applying FSIW-EFA. FSIW-EFA is a local rank analysis method designed to take into account the spatial structure of images [19]. Inspired in a previous algorithm used in process analysis [22], FSIW-EFA performs local Principal Component Analyses in the whole image by moving small windows around each individual pixel area. Each window is formed by a particular pixel and all its neighbors in the two spatial dimensions of the image (see Figure 2a). The number of pixels in the window should equal or exceed the total number of compounds in the image to allow for rank values representing all possible situations of compound overlap in the image. At the same time, it should be as small as possible to preserve the spatial resolution of the image and to discriminate better the pixel-to-pixel rank differences. In this example, a (2×2) window was used because the total number of image compounds is known to be four. The singular values obtained in these local analyses are displayed together in singular value plots where the spatial structure of the image is preserved (Figure 2b). In these plots, large values represent significant contributions to the signal, related to the presence of chemical constituents, whereas small values describe the experimental noise. Local rank maps are derived from the singular value plots by displaying the number of significant singular values in each pixel area. A threshold value or a threshold band is set to mark the limit between significant and noise-related singular values (see original reference for more details about threshold selection [19]). Depending on the threshold selection and on the information sought, we can distinguish between complete local rank maps (Figure 2c) and partial local rank maps (Figure 2d).

Complete local rank maps are obtained using a threshold value and show a rank value per pixel. The picture provides complete information on the local image complexity, that is, on how many constituents overlap in each pixel area (rank value). Figure 2c shows the complete local rank map for the emulsion image. According to the colors in the map, few selective pixels exist (blue) and most pixels contain mixtures of components, with rank two (green) in the center of the drop or in zones where the background phase is dominant and with higher rank values of three (orange) or even four (deep red) in the interphase zone between the drops or particles and the emulsion background. This complete local rank map already suggests how difficult the resolution of the image will be and which zones (pixels) present a higher complexity. Obviously, Figure 2c would present small changes if threshold values are slightly different to that selected. For exploratory purposes, this is not a relevant issue but, when resolution is intended and the rank value of a pixel is a crucial parameter to set constraints, a more careful estimation of the rank should be carried out.

Partial local rank maps are derived using a threshold band instead of a threshold value. The threshold band marks the lowest and highest boundaries for sensible threshold values. The only pixels shown in the partial local rank map are those whose rank is invariant within the threshold boundaries, that is, the pixels with the most robust rank estimation, the least threshold-dependent. The threshold band can be as wide as the user decides and the wider it is, the most restrictive is the pixel selection. Figure 2d shows the partial local rank map of the emulsion image. As can be seen, there are many voids in the image and the number of pixels with the most extreme rank values, one and four, have decreased significantly. Only the pixels in the partial local rank map, that is, those with the most reliable rank estimation, might be potentially constrained.

3.2. Image resolution

The resolution of the emulsion image has been carried out using the Multivariate Curve Resolution-Alternating Least Squares method (MCR-ALS) [4,22–24]. MCR-ALS is an iterative resolution method that has found wide application in data sets of different origins (processes, environmental, -omics,. . .) and of different structures (two-way to three-way and multiset arrangements)

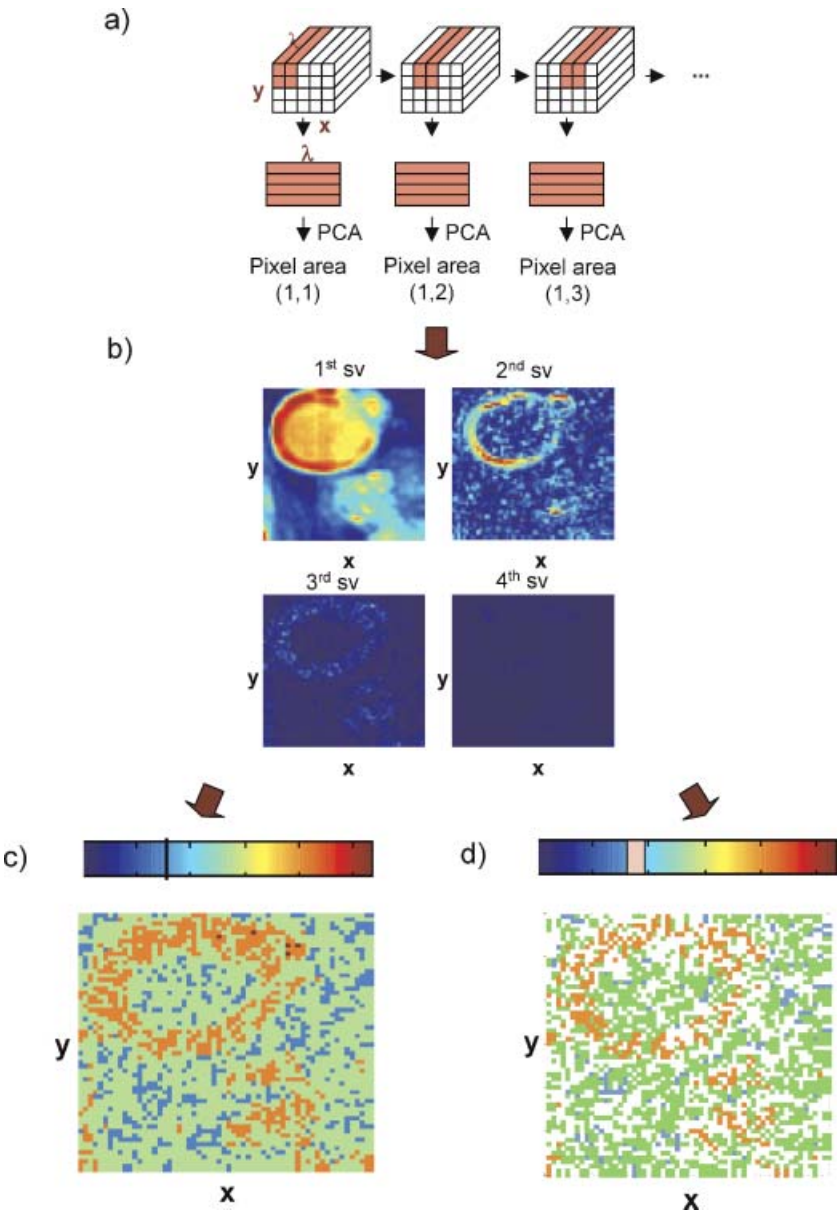

Figure 2. FSIW-EFA modus operandi. (a) Construction of image moving windows on 2D image structure. (b) Singular value plots from PCAs of individual pixel areas (from cold to hot colors, increase of s.v. scale). (c) Complete local rank map. (d) Partial local rank map. (For (c) and (d), rank 1 pixels in blue, rank 2 in green, rank 3 in orange and rank 4 in deep red). This figure is available in color online at www.interscience.wiley.com/journal/cem

[4,23–25]. Recently, we can find examples of application of MCR-ALS to the analysis of a single spectroscopic image [7,12–14] or to the simultaneous analysis of a series of images [9].

As any resolution method, the main goal of MCR-ALS is decomposing the matrix **D** of a multicomponent system into the underlying bilinear model

$$\mathbf{D} = \mathbf{C}\mathbf{S}^{\mathbf{T}} + \mathbf{E}$$

where **C** is the matrix of concentration profiles, $\mathbf{S}^{\mathbf{T}}$ the matrix of pure responses (often, spectra) and **E** contains the experimental error. In resolution of spectroscopic images, **D** is the matrix of the unfolded image, as in Figure 1a, **C** has the stretched pure concentration profiles that, conveniently refolded, show the distribution maps of each image constituent and $\mathbf{S}^{\mathbf{T}}$ contains their pure spectra (Figure 1c).

MCR-ALS works following the next general steps:

1. Determination of the rank of the data matrix **D**.
2. Generation of initial estimates (**C**-type or $\mathbf{S}^{\mathbf{T}}$-type).
3. Given **D** and **C**, constrained least squares calculation of $\mathbf{S}^{\mathbf{T}}$.
4. Given **D** and $\mathbf{S}^{\mathbf{T}}$, constrained least squares calculation of **C**.
5. Reproduction of **D** from calculated $\mathbf{C}\mathbf{S}^{\mathbf{T}}$. If reproduction is satisfactory, end of the process. If not, go back to 3.

The quality in data reproduction is evaluated by the lack of fit parameter, calculated as follows:

$$\text{lack of fit}(\%) = 100 \times \sqrt{\frac{\sum (d_{ij}^{*} - d_{ij})^2}{\sum d_{ij}^2}}$$

where d_{ij} is an element of the experimental matrix **D** and d^*_{ij} the element of the reproduced matrix by the MCR-ALS model, $\mathbf{CS}^T$.

Below, we will comment on the particularities of these steps related to the resolution of spectroscopic images through the analysis of our emulsion example.

Typically, spectral initial estimates are used to start the MCR-ALS optimization in the resolution of spectroscopic images. SIMPLISMA was applied to select the purest pixel spectra in the image to form the initial $\mathbf{S}^T$ matrix [5], although similar methods can be used for the same purpose.

Constraints are key elements in the iterative methods and they can be defined as mathematical or chemical properties that pure component profiles obey. The most applied constraint in image analysis is non-negativity in the concentration (pixel) direction and, when appropriate, in the resolved spectra. Because of the lack of a global continuous smooth evolution in the concentration profiles, typical process-related constraints, such as unimodality, closure or hard-modeling, cannot be used.

Local rank constraints introduce information on profile windows where all species but one are absent (selectivity) or, simply, on profile windows where some species are missing (local rank information) [4,17,18,23]. Typically, they are applied in the concentration direction and they are mainly responsible for the decrease or, often, suppression of rotational ambiguity in the resolution results [17,26]. In processes, the detection of concentration windows with a rank lower than the total can be easily done with local rank analysis methods, such as Evolving Factor Analysis, EFA [27], or Fixed Size Moving Window-Evolving Factor Analysis, FSMW-EFA [22]. Because of the sequential emergence-decay character of the concentration profiles in many processes, it is also quite straightforward to identify which components are absent in a particular window, for example in a selective window in the beginning of a process, all components but the one in the initial solution are absent.

The application of local rank constraints to images presents several problems. First, the correlated information in the concentration direction extends in the two spatial dimensions of the image and, therefore, applying methods designed for a single process direction, such as EFA or FSMW-EFA, would not work in the unfolded image data matrix, **D**. This inconvenience has been solved with the adapted algorithm FSIW-EFA. Second, the lack of a global patterned distribution of the constituents in an image, that is, the lack of concentration profiles with continuous or sequential behaviors, excludes the identification of the absent components in particular pixels from the sole information of the pixel rank.

In the introduction of local rank information constraints for image analysis, several aspects have been taken into account. As in the application of any other constraint, flexibility is a relevant issue. In this context, this means that we are not forced to constrain all pixels in an image, only those with very well defined information in terms of rank estimation and identification of missing components. We consider pixels with a reliable rank estimation those present in the partial local rank map (see Figure 3a). From all these pixels, only the ones with a rank lower than the total rank, four in this case, may potentially include selective or local rank information.

The identification of the missing components in a pixel requires confronting the pixel rank information with some reference spectral information. As mentioned before, the sole local rank information coming from the FSIW-EFA algorithm does not allow for a straightforward setting of constraints in the image because the distribution pattern of constituents is not sequential and cannot be known beforehand. In this example, this reference information comes from SIMPLISMA (see Figure 3b). From the four spectra selected, three of them (green, red and cyan) relate to drop constituents and the blue one, noisier because of the weak original spectral signal, represents the background phase. At this point, we should stress that the reference spectral information can come from other pure variable selection methods, from the resolved $\mathbf{S}^T$ matrix in a prior MCR-ALS application using only non-negativity constraints and, obviously, from the combination of any of the possibilities above with some real pure spectra when the nature of some of the constituents in the image is known. Nevertheless, the use of a pure variable method, such as SIMPLISMA, to obtain reference spectral information is not a problem. Even if there are no selective pixels in the image, the selected spectra will be the best representations of the different constituents within the image and, therefore, useful for the identification of missing components in other pixels.

The incorporation of local rank constraints in any pixel starts estimating the number of missing components in the pixel. Thus, for any pixel *i* in Figure 3a,

$$\text{nr. missing components}(i) = \text{image total rank} - \text{local rank pixel}(i)$$

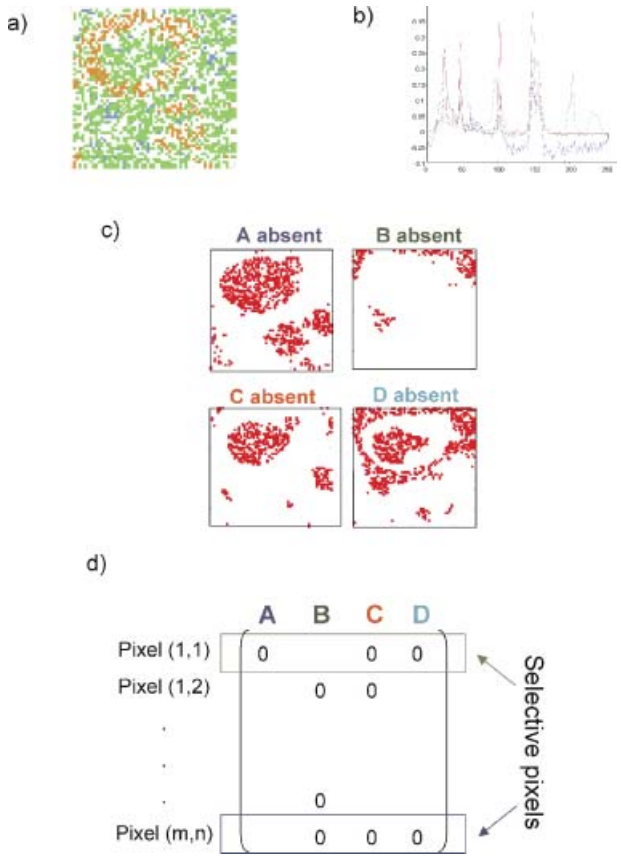

Figure 3. Setting of local rank constraints in the emulsion image. (a) Partial local rank map (as in Figure 2d). (b) Reference spectral information (pure spectra selected by SIMPLISMA). Blue: background (A); green: inner drop component (B); red: interphase component (C) and cyan: minor additive component (D). (c) Plots of missing component pixels. (d) Translation of (c) plots into a matrix with local rank information (**csel**). This figure is available in color online at www.interscience.wiley.com/journal/cem

for example, for a pixel of rank three, we should look for one missing component. The way to identify this component passes through the calculation of the correlation coefficient between the raw pixel spectrum and each one of the reference spectra (Figure 3b). The component with the lowest correlation coefficient with the pixel spectrum will likely be the one missing in this pixel. This procedure is done individually for each of the pixels that can be potentially constrained. Figure 3c shows the absent components identified for the pixels in Figure 3a. Please note that the shape of the missing areas matches the nature of the compounds in the image. Thus, compound labeled A refers to the background, B is the major compound in the inner part of the drop, C is the main compound in the outer part of the drop and D refers to an additive present in localized zones of the sample. In pixels where more than one component is absent, the reference spectra showing the smallest correlation coefficients with the pixel spectrum will be the missing ones. The use of the correlation coefficient for identification of missing compounds in a pixel has been proposed because it allows to work individually with each pixel. Other typical identification methods, such as target testing strategies, would need to work with a pixel and its surrounding area (several spectra) to build a suitable image subspace, where the reference spectra would be projected. Since constraints should be set on individual pixels, these methods have been discarded.

At this point, we need to consider that the identification of the missing components may not always be conclusive enough. To prevent the introduction of misidentifications, the first step consists of seeing the natural correlation between the spectra used as reference (see matrix below for this example).

$$\begin{array}{c} \\ A \\ B \\ C \\ D \end{array} \begin{array}{c} \begin{array}{cccc} A & B & C & D \end{array} \\ \begin{pmatrix} 1 & 0.58 & 0.75 & 0.52 \\ 0.58 & 1 & 0.66 & 0.67 \\ 0.75 & 0.66 & 1 & 0.61 \\ 0.52 & 0.67 & 0.61 & 1 \end{pmatrix} \end{array}$$

Thus, the absence of a particular component in a pixel will not be confirmed unless the correlation coefficient between the pixel spectrum and the reference spectrum of that component be equal or smaller than the largest element in the correlation matrix for that particular component. In this concrete example, A cannot be considered a missing component if the correlation coefficient obtained with the pixel spectrum is larger than 0.75. The highest acceptable correlation coefficients to consider B, C and D missing will be 0.67, 0.75 and 0.67, respectively. Therefore, even a pixel with a well-defined rank will not be constrained unless a reliable identification of the missing components is achieved. In this example, only 1177 pixels have been constrained, even though the number of pixels in the partial local rank map is 1934. The total number of pixels in the image is 3600. It is important to remember that the reliable identification of the missing components in a pixel is achieved through the combination of local rank and reference spectral information. Using only one of the two sources of information would be either insufficient (local rank in itself only tells about the number of missing components in a pixel) or overtly dangerous (a low correlation coefficient between a pixel spectrum and a reference spectrum can indicate either that the reference component is missing or is a minor compound. Complementary rank information is needed to find out which is the real answer).

To finish the process of implementation of local rank constraints, the information accepted in terms of rank and compound identification is translated into a 'mask' matrix (Figure 3d). This matrix, sized as **C** (nr. of pixels $\times$ nr. of components), will be used to introduce the local rank constraints in the resolution process. It is the so-called **csel** matrix in the MCR-ALS graphical user interface designed by the authors [23]. Local rank constraints can be applied keeping null values in the concentration elements of the missing components in the constrained pixels (equality constraint) but, in practice, better results are obtained if these missing components are set to have a concentration value equal or smaller than a very small predefined value (inequality constraint) [4,17,28].

Figure 4 shows the resolution results for the emulsion sample using only non-negativity constraints (Figure 4a) and non-negativity and local rank information (Figure 4b). The lack of fit in both analyses is 7.8% and 8.7%. The similarity of both values indicates that the constraints introduced are correct and do not perturb the natural behavior of the data set. Although the

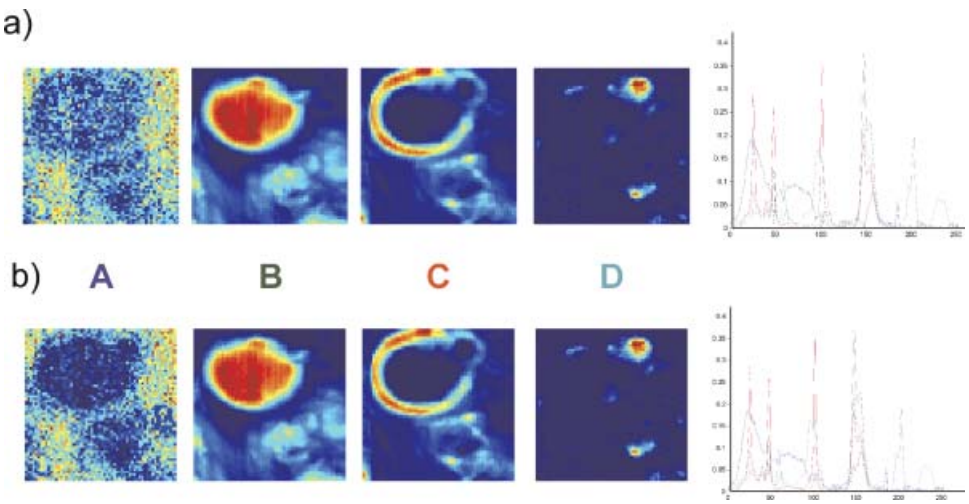

Figure 4. (a) Image resolution applying non-negativity constraints in the concentration and spectral directions. Distribution maps and pure spectra. (b) The same as (a) including also local rank constraints in resolution. This figure is available in color online at www.interscience.wiley.com/journal/cem

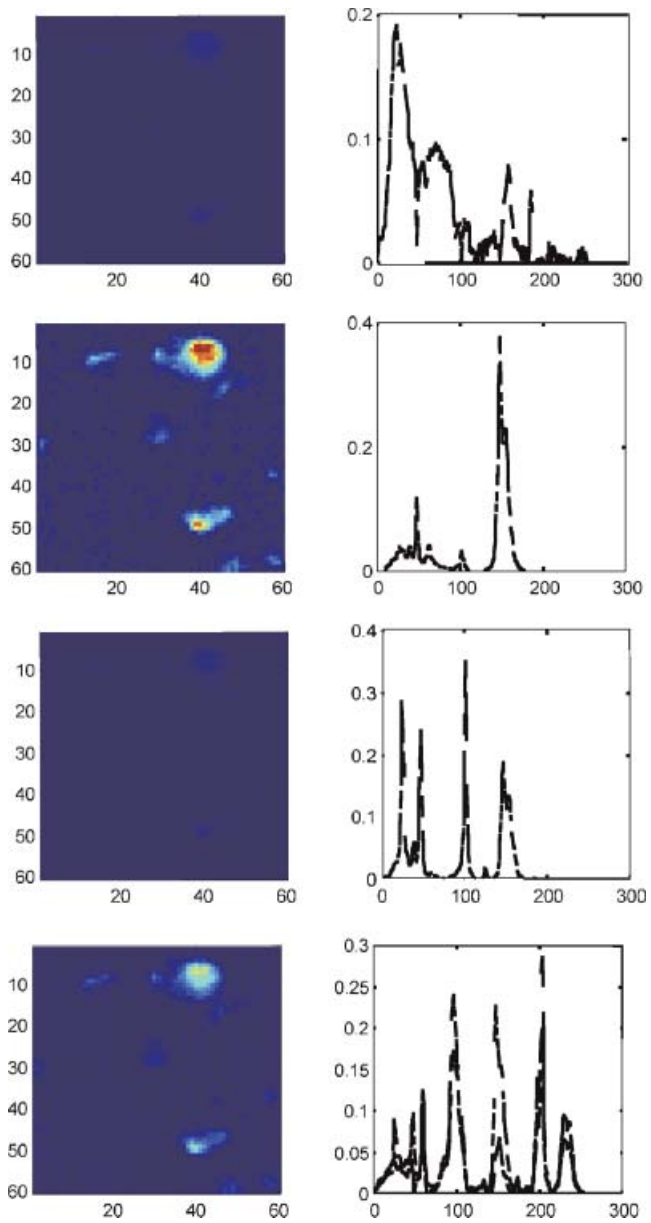

Figure 5. Ambiguity in the resolution results for A, B, C and D components (from top to bottom) when applying only non-negativity constraints. For each component, left plot: refolded 2D representation of $\mathbf{c}_{i,max} - \mathbf{c}_{i,min}$; right plot: overlaid plot of $\mathbf{s}_{i,max}$ and $\mathbf{s}_{i,min}$. This figure is available in color online at www.interscience.wiley.com/journal/cem

distribution maps and spectra look very similar in Figure 4a and b, there is a more neat definition of the components, particularly from the background, in Figure 4b.

Another parameter that may help to understand the benefit of introducing local rank information is the assessment of the ambiguity in the recovered profiles. As we mentioned before, the effect of constraints is a key factor for the decrease or even suppression of the rotational ambiguity in the resolution results. To assess the uncertainty linked to the recovered profiles, we have used Tauler's method to obtain the minimum and maximum boundaries of the feasible solution bands [28]. These boundaries are calculated for each constituent *i* and they are represented by two dyads of spectrum/concentration profile giving a maximum ($\mathbf{c}_{i,max}\mathbf{s}_{i,max}^T$) and minimum ($\mathbf{c}_{i,min}\mathbf{s}_{i,min}^T$) signal contribution in the reproduction of the data set and obeying the preselected constraints.

Figure 5 displays information on the feasible solution bands obtained from the resolution of the emulsion image using only non-negativity constraints. For each image constituent, the plots on the right show overlaid representations of the maximum and minimum spectral boundaries, $\mathbf{s}_{i,max}$ and $\mathbf{s}_{i,min}$ (these boundaries overlap in some components and appear as a single profile). For a better visualization of the ambiguity in the distribution map, the plots in the right display the difference between $\mathbf{c}_{i,max}$ and $\mathbf{c}_{i,min}$. (for better comparison, the same absolute color scale has been used in all distribution maps). Different components show variable degrees of ambiguity in the concentration and/or spectral direction. Thus, major compounds A, B and C hardly present ambiguity in the spectral direction, probably due to the presence of selective or almost selective pixels in the image with very well defined spectral shapes. In contrast, they have ambiguity in a major or minor extent in the concentration direction, likely due to the larger overlap among components in the spectral direction. The minor additive component (D) is the one showing more ambiguity because of the higher overlap with the rest of constituents in either direction.

The positive effect of local rank constraints is clearly seen when we calculate the feasible solution bands for the resolution of the emulsion image incorporating this new constraint. The profiles resolved are unique and, therefore, no feasible solution bands exist. Actually, this is not an isolated example. Apparently negative features of all image data sets, such as the large size and the unpatterned concentration profiles, really help for resolution purposes. Thus, the huge number and variety in the combination of missing components in pixels makes that including this information under the explicit form of local rank constraints ensures very frequently the uniqueness in the resolved image profiles.

4. CONCLUSIONS

A way has been provided to incorporate local rank constraints for image resolution. To do so, a combination of an image-oriented local rank method and some reference spectral information is needed for a proper estimation of the pixel rank and identification of the missing components. The use of this constraint results in better defined image profiles and, most of the times, in the suppression of the ambiguity in the results obtained.

REFERENCES

1. Hornak JP. Encyclopedia of Imaging Science and Technology. Wiley: New York, 2002.
2. Geladi P, Grahn H. Multivariate Image Analysis. John Wiley & Sons Ltd.: Canada, 1997.
3. de Juan A, Casassas E, Tauler R. Soft modeling of analytical data. In Encyclopedia of Analytical Chemistry: Instrumentation and Applications. John Wiley & Sons: Chichester, UK, 2000; 9800.
4. de Juan A, Tauler R. Chemometrics applied to unravel multicomponent processes and mixtures. Revisiting latest trends in multivariate resolution. *Anal. Chim. Acta* 2003; **500**: 195–1210.
5. Windig W, Guilment J. Interactive self-modeling mixture analysis. *Anal. Chem.* 1991; **63**: 1425–1432.
6. Dupuy N, Batonneau Y. Reliability of the contribution profiles obtained through the SIMPLISMA approach and used as reference

in a calibration process—application to Raman micro-analysis of dust particles. *Anal. Chim. Acta* 2003; **495**: 205–215.
7. Duponchel L, Elmi-Rayaleh W, Ruckebusch C, Huvenne JP. Multivariate curve resolution methods in imaging spectroscopy: influence of extraction methods and instrumental perturbations. *J. Chem. Inf. Comput. Sci.* 2003; **43**: 2057–2067.
8. Berman M, Miiveri H, Lagerstrom R, Ernst A, Dunne R, Huntington JF. ICE: a statistical approach to identifying endmembers in hyperspectral images. *IEEE Trans. Geosci. Remote Sensing* 2004; **42**: 2085–2095.
9. de Juan A, Tauler R, Dyson R, Marcolli C, Rault M, Maeder M. Spectroscopic imaging and chemometrics: a powerful combination for global and local sample analysis. *TrAC-Trends Anal. Chem.* 2004; **23**: 70–79.
10. Wang JH, Hopke PK, Hancewicz TM, Zhang SLL. Application of modified alternating least squares regression to spectroscopic image analysis. *Anal. Chim. Acta* 2003; **476**: 93–109.
11. Wentzell PD, Karakach TK, Roy S, Martínez MJ, Allen CP, Werner-Washburne M. Multivariate curve resolution of time course microarray data. *BMC Bioinformatics* 2006; art.343.
12. Sobanska S, Falgayrac G, Laureyns J, Bremard C. Chemistry at level of individual aerosol particle using multivariate curve resolution of confocal Raman image. *Spectrochim Acta A Mol Biomol Spectrosc* 2006; **64**: 1102.
13. Zhang L, Henson MJ, Sekulic SS. Multivariate data analysis for Raman imaging of a model pharmaceutical tablet. *Anal. Chim. Acta* 2005; **545**: 262–278.
14. Budevska BO, Sum ST, Jones TJ. Application of multivariate curve resolution for analysis of FT-IR microspectroscopic images of *in situ* plant tissue. *Appl. Spectrosc.* 2003; **57**: 124–131.
15. Hancewicz TM, Wang J-H, Pudney PDA, Zhang SL. *Multivariate image resolution for spectroscopic image analysis*. 228th ACS National Meeting, Philadelphia, PA, August 22 2004; Paper 15.
16. Hancewicz TM, Wang JH. Discriminant image resolution: a novel multivariate image analysis method utilizing a spatial classification constraint in addition to bilinear non-negativity. *Chemom. Intell. Lab. Syst.* 2005; **77**: 18–31.
17. Tauler R, Smilde AK, Kowalski BR. Selectivity, local rank, 3-way data-analysis and ambiguity in multivariate curve resolution. *J. Chemom.* 1995; **9**: 31–58.
18. Geladi P, Wold S. Local Principal Component Models, rank maps and contextuality for curve resolution and multi-way calibration inference. *Chemom. Intell. Lab. Syst.* 1987; **2**: 273–281.
19. de Juan A, Maeder M, Hancewicz T, Tauler R. Local rank analysis for exploratory spectroscopic image analysis. Fixed Size Image Window-Evolving Factor Analysis. *Chemom. Intell. Lab. Syst.* 2005; **77**: 64–74.
20. Andrew JJ, Browne MA, Clark IE, Hancewicz TM, Millichope AJ. Raman imaging of emulsion systems. *Appl. Spectrosc.* 1998; **52**: 790–796.
21. Andrew JJ, Hancewicz TM. Rapid analysis of Raman image data using two-way multivariate curve resolution. *Appl. Spectrosc.* 1998; **52**: 797–807.
22. Keller HR, Massart DL. Peak purity control in liquid chromatography with photodiode array detection by fixed size moving window evolving factor analysis. *Anal. Chim. Acta* 1991; **246**: 379–390.
23. Tauler R. Multivariate curve resolution applied to second order data. *Chemom. Intell. Lab. Syst.* 1995; **30**: 133–146.
24. Jaumot J, Gargallo R, de Juan A, Tauler R. A graphical user-friendly interface for MCR-ALS: a new tool for multivariate curve resolution in MATLAB. *Chemom. Intell. Lab. Syst.* 2005; **76**: 101–110.
25. de Juan A, Tauler R. MCR from 2000: progress in concepts and applications. *Crit. Rev. Anal. Chem.* 2006; **36**: 163–176.
26. Manne R. On the resolution problem in hyphenated chromatography. *Chemom. Intell. Lab. Syst.* 1995; **27**: 89–94.
27. Maeder M. Evolving Factor Analysis for the resolution of overlapping chromatographic peaks. *Anal. Chem.* 1987; **59**: 527–530.
28. Tauler R. Calculation of maximum and minimum band boundaries of feasible solutions for species profiles obtained by multivariate curve resolution. *J. Chemom.* 2001; **15**: 627–646.

